The thermo-mechanical impact of long-term energy pile use

Rafai, Mouadh; Salciarini, Diana; Vardon, Philip J.

DOI
10.1016/j.renene.2025.122693

Publication date
2025

Document Version
Final published version

Published in
Renewable Energy

Renewable Energy 244 (2025) 122693

Contents lists available at ScienceDirect

Renewable Energy

journal homepage: www.elsevier.com/locate/renene

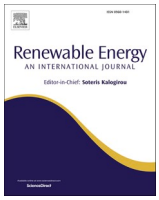

The thermo-mechanical impact of long-term energy pile use

Mouadh Rafai [a,b,*], Diana Salciarini [a], Philip J. Vardon [b,**]

[a] Department of Civil and Environmental Engineering, University of Perugia, via G. Duranti, 06125, Perugia, Italy
[b] Faculty of Civil Engineering and Geosciences, Delft University of Technology, 2628CN, Delft, the Netherlands

ARTICLE INFO

Keywords:
Energy pile
Bearing capacity
Full-scale field tests
Long-term monotonic cooling conditions
Thermo-mechanical response

ABSTRACT

This paper presents quantitative data from a field test on a new type of energy pile, called a displacement cast in situ energy pile. The test pile was installed in a multilayered soft soils and subjected to a continuous cooling for 3 months, with no mechanical load. Afterwards, the pile was loaded to a specific target of 20 or 60 % of its calculated ultimate bearing capacity and then subjected to up to five thermal cycles. Under zero mechanical load, the results revealed that the compressive/tensile stresses coexist along the pile. Under low mechanical load (20 %), thermal cycles induced irreversible residual contractive strains and stresses as well as a limited pile head settlement. Under high mechanical load (60 %) and extreme operating conditions, i.e., negative temperatures which could have indicated a frozen interface, further irreversible settlements observed at the end of this test. Mechanical pile tests however indicated no impact of stress history (including the freezing test) on the shaft resistance and the overall pile-bearing capacity.

1. Introduction

Heat supply for space heating or domestic hot water in buildings is mainly provided by individual heat sources (e.g., boilers) or by district heating networks (DHN). The key advantages of DHNs over individual heat sources include delivering heat more efficiently, cheaply and with lower carbon emissions [1]. These systems are currently used noticeably in countries with cold climates such as Scandinavia, Eastern Europe, and Russia [1]. For instance, 90 % of the housing in Iceland is heated via district heating networks distributing hot water sourced from geothermal energy [2]. Energy geostructures, i.e., piles, walls and tunnels, are a type of shallow geothermal energy, where in-ground structures are equipped with heat exchanger pipes. These pipes are connected to a ground source heat pump (GSHP) extracting thermal energy from the ground to building in the winter and vice versa in the summer [3]. Energy piles in particular are an innovative technology that combines geothermal heat exchange and structural foundation support. In energy piles, a major cost related to drilling for installation is saved compared to conventional borehole heat exchanger, because these structures are already in place to provide structural support. Moreover, this practice can be characterized by low maintenance, cost-effectiveness, long lifetime, less variation in energy supply compared to solar and wind power, and environmental friendliness [12]. Energy piles constructed as a part of GSHP systems have seen increased growth in markets and research in the last few years [4,5]. Such systems are suited for supplying low temperature DHNs, and in particular to close-by buildings in small scale grids. However, their wider potential to integrate into district heating networks lies in the fact that the thermo-mechanical response of these structures should be extensively tested through full-scale in situ tests in different conditions. During the ground source heat pump operations either continuous or intermittent operation, energy piles and the soil surrounding them are subjected to short-term (daily or even hourly) and long-term (seasonal) temperature changes. This may affect the surrounding soils (change in shear strength, excess pore water pressure generation, volumetric strains) and the pile itself (thermally induced axial stresses along the energy pile and change in mobilized shaft resistance). And even thermal creep at the soil-structure interface which may affect the superstructure [6,7]. Such operations apply additional thermally-induced mechanical loads, which can impact both the serviceability and failure of piles. Pile strains, stresses, and movements during heating and cooling are inevitable due to the thermal expansion/contraction of the soil and the pile, such consequences maybe permanent and can accumulate, inducing an impact on the bearing capacity of a pile [8,9]. Furthermore, these relative movements may alter

This article is part of a special issue entitled: Geothermal heating-cooling published in Renewable Energy.

* Corresponding author. Faculty of Civil Engineering and Geosciences, Delft University of Technology, Delft 2628CN, the Netherlands.
** Corresponding author. Faculty of Civil Engineering and Geosciences, Delft University of Technology, Delft 2628CN, the Netherlands.
E-mail addresses: mouaadrafai@gmail.com (M. Rafai), p.j.vardon@tudelft.nl (P.J. Vardon).

https://doi.org/10.1016/j.renene.2025.122693
Received 18 September 2024; Received in revised form 23 December 2024; Accepted 16 February 2025
Available online 17 February 2025

the shear transfer mechanism at the pile-soil interface. In recent years, researchers have extensively investigated the thermo-mechanical behavior of energy piles, through full-scale in situ tests (e.g., Refs. [3,10–30]), laboratory tests (e.g., Refs. [31–43]), and numerical modeling (e.g., Refs. [44–54]). Several field scale tests on instrumented energy piles have been performed during monotonic heating or cooling [13–15,16,17,25] and cyclic thermal loads [19–26]. Wang et al. [17] investigated the impact of short-term (9 days) and long-term (52 days) monotonic heating on the pile bearing capacity. It was observed that the increase in temperature during the heating periods prompted the pile shaft to expand radially. Subsequently, as the pile cooled down naturally, the pile shaft slowly contracted and returned closely to its original condition, suggesting a thermoelastic behavior. Note that the energy pile was installed in dry, very dense sand and clay [17]. Ren et al. [25] investigated the impact of cooling on the pile bearing capacity. Their results indicated a decrease in the pile bearing capacity which was attributed to the deformation between the pile and the soil due to the cold load. It should be noted that the duration of cooling in the study by Ren et al. [25] was only 120 h. Thus, the impact of long-term cooling on the pile capacity has received little attention, especially in soft soils. Soft soils tend to deform permanently due to thermal change [55,56,57]. In the case of energy piles in soft soils, the ground may deform further when the cooling extends further into the soil, and this may contribute to further apparent deformation of the pile [58].

Laboratory tests have shown ratcheting effects in heavily-loaded piles undergoing cyclic heating and cooling and even exceeded serviceability and ultimate criteria in the case of elevated pile groups while energy-piled rafts settlement remained within the acceptable range [8]. Similarly, this phenomenon has been observed through full-scale tests [28]. An experimental study conducted on small-scale models tested in a geotechnical centrifuge at 40 g has shown that an energy pile installed in lightly overconsolidated (OC) clay accumulates larger irreversible settlements if compared to a pile in heavily overconsolidated clay [58]. Although these studies provide an understanding of the pile response mechanisms with control of the studied variables and numerous thermal cycles can be applied in a relatively short time. However, in the field, ground conditions are more complex, especially in multilayered soft soil conditions. For this reason, it is necessary to carry out further studies to comprehensively analyze the potential effects of long-term monotonic thermal load on the interactions between energy piles and the surrounding soft soil. In cold-dominated climates, e.g., The Netherlands, there is likely to be more energy extracted than injected leading to net ground cooling. Jiang et al. [24] examined the thermo-mechanical behavior of driven energy piles subjected to varying mechanical loads during up to four thermal cycles. Their findings revealed that cooling-recovery cycles led to an elastic-plastic response of the pile at specific mechanical loading levels, with cooling-induced settlement significantly exceeding that caused by mechanical load. Additionally, Jiang et al. [29] investigated a long floating energy pile subjected to thermal cycles (cooling–natural heating and heating–natural cooling) under a constant mechanical load. Their results demonstrated notable permanent settlement, particularly under cooling conditions. Heating, on the other hand, induced a substantial increase in axial force which could reach up to four times greater than that observed under purely mechanical loading. While cooling reduced the stress initially caused by the applied mechanical load. The magnitude of the axial load variation was closely dependent on the temperature change. These studies collectively highlighted that cooling results in significant irreversible settlement, which could adversely impact the shaft capacity of energy piles. Kong et al. [26] reported that residual strains, stresses, and settlements developed during the thermal cycles, and persisted when the temperature was fully recovered after three thermal cycles. Recently, Rafai et al. [3] introduced a new type of energy pile called displacement cast in situ energy piles (as opposed to other studies which consider only non-displacement (cast-in-situ) and displacement (precast) piles) and it has been observed that their behavior differs from other types of energy piles, i.e, a high load was transferred to the shaft and there was only a minor impact of thermal cycles on the shaft resistance. This was attributed to the increase of shaft resistance of the pile as a result of the densification of the surrounding soils during the pile installation, which is beneficial for the shaft, especially in soft soils. Moreover, under higher mechanical load higher permanent strains and settlements along the pile were observed. In that test, the duration of the cooling load was also limited to 12 h. Therefore, the impact of long-term-monotonic cooling load has not been investigated and remains unclear.

Generally, the available full-scale research mostly focuses on the thermally induced strains and stresses [15,16,17,19,21–23], while fewer studies on the pile displacement [24,28,29], possibly due to the challenges encountered during mounting sensors on the pile head when the superstructure takes place. The assessment of effects thermal loads on strains, stresses, and pile head displacements using instrumented energy piles in field settings remains rare. Field studies are essential to comprehensively account for the combined effects of installation procedures, actual construction materials, subsurface stratigraphy, and boundary conditions at the pile head and toe. Therefore, incorporating these factors into the design of energy piles is crucial to avoid any exceedance in serviceability and ultimate criteria [19].

This paper investigates the thermo-mechanical behavior of a displacement cast in situ energy pile, i.e., Fundex energy piles, under long-term monotonic thermal load (up to three months without mechanical load) and cyclic thermal loads at two mechanical load levels (20 and 60 % of the pile bearing capacity), representing various operational scenarios of GSHP systems, including an extreme conditions (freezing) test. The thermally induced strains, stresses and pile head displacements are presented. The potential effects of the thermal load on the shaft capacity as well as on the overall pile capacity in a heating-dominant climate are discussed. This study aims to provide quantitative data on a displacement cast in situ semi-floating energy pile installed in multilayered soft soils, incorporated into a ground-source heat pump system.

2. Review of the case study details

Rafai et al. [3] provide detailed information including the installation method of the full-scale displacement cast-in-situ energy pile, constructed for this research in Delft, The Netherlands. The installation of this type of energy piles was made in three phases. i) During the drilling phase, a steel casing with a conical auger tip i.e., a Fundex cone, at its base is rotated down into the soil, compacting the adjacent ground. ii) In the second phase, a reinforcement cage incorporating the heat exchanger loops is inserted into the casing, which is then filled with concrete. iii) in the last phase, the Fundex cone is subsequently detached from the casing, allowing the casing to be withdrawn. The sacrificial tip remains in place, forming an expanded pile base. In this study, the energy pile with two high-density polyethylene (HDPE) pipe closed loop heat exchangers in a “double-U” configuration (U-loops) was investigated to provide further quantitative data on the thermo-mechanical response in multilayered soft soil. The energy pile was fully instrumented to monitor its thermo-mechanical response. Twelve Vibrating Wire Strain Gauges (VWSGs) with integrated thermistors were installed along the pile to measure both strain and temperature variations. Additionally, a Linear Variable Differential Transformer (LVDT) with an integrated thermistor was utilized to monitor the pile head displacement and air temperature. The locations of the strain gauges along the pile depth are indicated in Fig. 1, referring to the average depth of the two strain gauges, i.e. the position of the thermistor. The strain gauges were used to assess the effects of the thermo-mechanical load on the pile shaft and the LVDT was mounted on the top of the pile to measure the pile head displacements. The mechanical load at the pile head was applied via dead weight by means of a hydraulic jack that was used to develop a compressive force on the pile head, coupled with one load cell placed

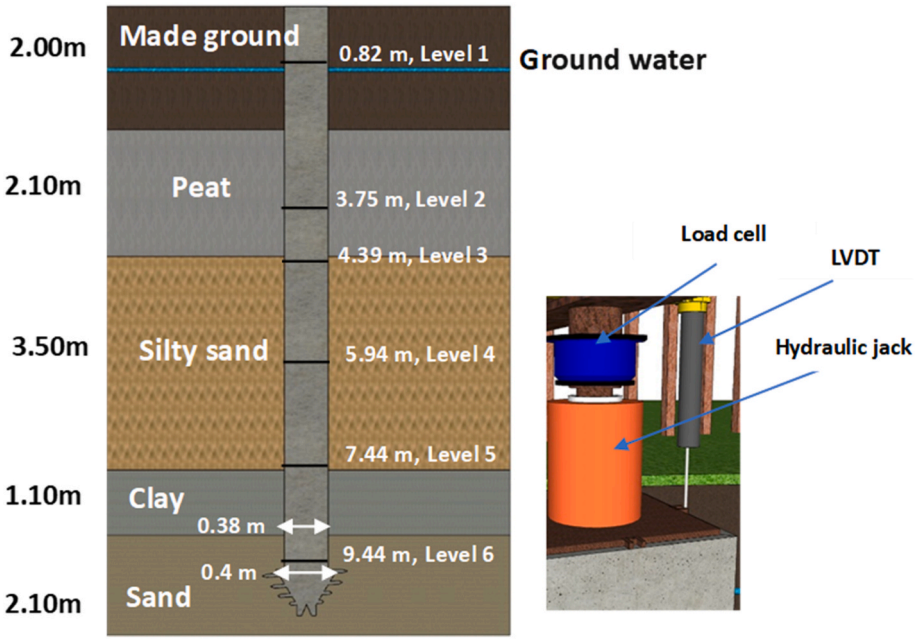

Fig. 1. Schematics of the energy pile including locations of instrumentation.

between the jack and the frame to record and control the applied load (see Fig. 1). A GSHP was connected to the pile to circulate the heat exchange fluid which was a mixture of 30 % monoethylene glycol and 70 % water by volume. All the instrumentation was connected to a data logger system to record continuous measurements along the pile shaft and pile head with a time interval of 1 min.

Cone penetration tests (CPTs) were conducted to investigate the site stratigraphy. The ground at the site consists of a shallow made ground, underlain by 2.1 m of highly organic clay (i.e. peat). With increasing depth, a silty sand layer ranges from 4.1 m to 7.6, followed by a 1.1 m thick clay. Underneath this lies a layer of sand extending from 8.7 m to 12.0 m. The test site features soft soil conditions typical of the western Netherlands with tip resistance qc values of 0.2–10 MPa [3]. The tip resistance from CPT data and average thermal property data (averaged from CPT correlations [59] and needle probe tests) are summarized in Table 1.

The pile shank diameter was 380 mm while the tip diameter was 400 mm; forming an expanded tip, which was positioned at a depth of 10.3 m in sandy soil. The groundwater was located at a depth of 1 m below the ground surface (Fig. 1). The initial ground temperature was approximately 12 °C below the depth of 4 m.

3. Experimental scheme

The experimental program was designed to cover several scenarios of GSHP operations and to represent the energy consumption patterns in the Netherlands, which is mostly heating the building (cooling down the pile). It should be noted that before this testing program, the pile had been subjected to thermal cycles and allowed to recover [3].

The testing schedule, as shown in Table 2, includes five testing phases: Two mechanical load tests (before and after the thermo-mechanical tests), a long-term thermal test, and two shorter periods of thermo-mechanical testing at different mechanical loads.

Table 1
Thermal and mechanical parameters.

Proprieties	Made ground	Peat	Silty sand	Clay	Sand
Tip resistance (MPa)	0.2–14	0.3	3	0.8	6–10
Heat capacity mJ/(m3·K)	1.5	0.9	2.8	2.3	2.4
Thermal conductivity W/(m·°C)	1.1	0.54	1.6	1.4	1.9

Table 2
Test program.

Test No.	Mode	Cycle	Cooling/Natural-heating duration	Static load (kN)
T_M1	Mechanical	_	_	0, 36, 71, 106, 141, 176, 211
T_0	Thermal	1	3 months	0
T_20	Mechanical + thermal	4	4 days	71
T_60	Mechanical + thermal	1	5 days	211
T_M2	Mechanical	_	_	0, 36, 71, 106, 141, 176, 211

The testing program was designed to reflect varying specific operating conditions of the GSHP system. In test T_0, the GSHP operated naturally without any imposed changes in the heat pump operation. This test also ensured that the surrounding soil was sufficiently cooled in order to make later test periods where more extreme temperatures were required easier. In the other tests, the duration of thermal cycles was gradually reduced while their magnitude was increased to investigate the system's response under more intensive thermal loading, which may exist for shorter periods in real world applications.

The predicted bearing capacity was calculated to be 353 kN. In the first test phase (T_M1), the pile was loaded up to 0.6 Q_{max} (60 % of the estimated bearing capacity) with increments of 0.1 Q_{max} (10 %), each loading steep was maintained for at least 60 min. Afterwards, the pile was unloaded. For the mechanical tests, incremental loading according to the procedure recommended by the Dutch code for static axial loading of piles [60] was adopted. During mechanical loading tests, load settlement stability was assessed using mechanical creep measurements. Specifically, the mechanical creep was monitored using LVDT data over the final 15 min of each load step. If the mechanical creep was less than 0.75 mm within this 15-min period, the next loading step was applied. During the second test phase (T_0), a long-term free-expansion test was conducted with no load applied to the pile with an average temperature variation of approximately 5 °C.

During the third and fourth phases, two thermo-mechanical tests,

T_20 and T_60, were conducted under two mechanical load levels, 20 %, and 60 % of the estimated bearing capacity, respectively. In these tests, the pile was loaded to the desired target and then maintained for a duration of 16 h to minimize the creep effects, and then thermal loads of cooling-natural heating were applied.

In test T_20, four thermal cycles were applied, while in test T_60, one thermal cycle was applied. The average temperature variations were approximately 10 °C and 11 °C in tests T_20 and T_60, respectively. This high-temperature magnitude may represent a high heating demand in cold winters, or maybe when the system fails, in such cases continuous heat extraction could be resulted, and thus a high magnitude of temperature change in the pile and may lead to a frozen interface. The test T_60 aims to explore this possibility and its consequences. The first step to define the thermal effects is to isolate the effect of the mechanical loading. The strain and pile head displacement due to purely mechanical load (i.e., after 16 h), is considered to be constant, assuming that there is negligible creep effect due to load applied to the pile head over time. Accordingly, the measured strain and pile head displacement values ($\varepsilon_{meseared}$) were zeroed by subtracting the mechanical axial strain and pile head displacement, then, the results due to the temperature variations can be interpreted. In the final phase (T_M2), and after the thermal recovery, another mechanical test was carried out exactly as the first one, up to 0.6Qmax (60 %), by the increments of 0.1Qmax (10 %) to assess the impact of stress history on the bearing capacity.

4. Full-scale in-situ test results and analysis

The post-processing methodology of the recorded data is detailed by Rafai et al. [3].

4.1. Mechanical behavior with no heating or cooling

Fig. 2(a) and (b) present the profiles of the axial stress and the distribution of pile mobilized shaft resistance along pile depth under different mechanical load conditions, respectively, obtained from the static load tests T_M1 and T_M2, before and after thermo-mechanical tests. Fig. 2(c) exhibits the curves of pile head displacement versus the applied load, obtained from these two mechanical tests.

The application of mechanical load to the pile head tends to cause a relative displacement between the pile and the soil. Therefore, the pile behavior was affected by shaft friction resistance, causing a gradual reduction in axial stress. The axial stress, shaft resistance and pile head displacement increased with increased applied mechanical load. The maximum and minimum shaft resistance were obtained at zone C (from 3.75 to 4.39 m) m and zone 1 (from 0 to 0.82 m), respectively, being 32 kPa and −5 kPa, respectively, under a load of 211 kN.

The shaft resistance generally decreases with depth consistent with the reduction in applied load seen in Fig. 2(a), with increases where the soil changes to a stiffer layer. The shaft resistance in zone A of the pile body is the smallest. For example, approximately 4 and -1 kPa were observed in tests T_M1 and T_M2 respectively under the same loading step 211 kN. This is probably due to the lowest restraining effect by the made ground layer along with its possible deformation during the mechanical load. Similarly, this can explain the negative value of −0.26 kPa under the lowest applied mechanical load (71 kN) in zone D (4.39–5.94 m), and possibly preexisting stress at level 4. In both tests, under the same level of static load, the axial stresses of the two mechanical tests under the applied mechanical loads are quantitatively identical. This indicates that the shaft resistance between test T_M1 and

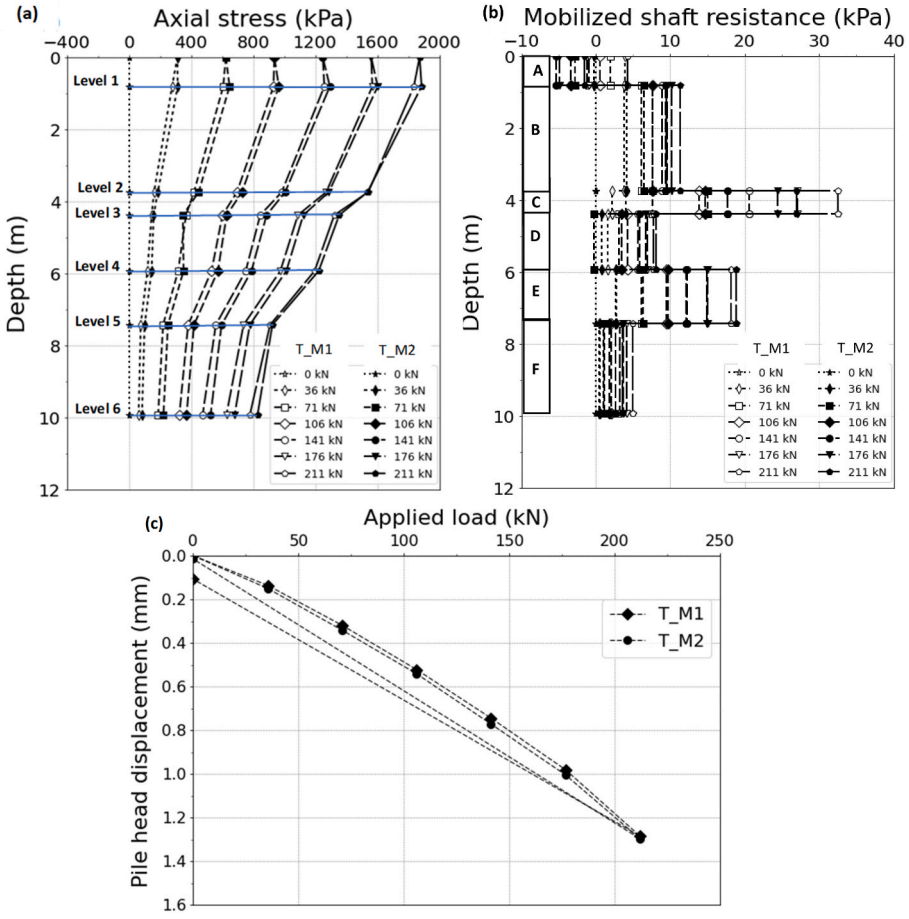

Fig. 2. Mechanical response of energy pile obtained from test T_M1 test: (a) Axial strain and force at each level, (b) mobilized shaft friction versus the depth at each zone, and (c) pile head displacement versus the applied mechanical load.

T_M2 remains largely unaffected (e.g., see the slopes from pile top to level 1 or from level 3 to level 4, of the two tests in Fig. 2(a)), implying a negligible impact on unit shaft resistance along the pile length, with the mobilized shaft resistance shown in Fig. 2(b).

As seen in Fig. 2(c), the results of pile head displacements are nearly identical for 10, 20, 30, 40, 50 and 60 % of the estimated bearing capacity in each test.

A pile head displacement of approximately 1.2852 mm in both tests T_M1 and T_M2 corresponding to 0.34 % of the pile diameter under 60 % of the estimated bearing capacity. This indicates that the pile bearing capacity remains constant. After unloading the pile in both tests, the results of the pile head displacements due to the mechanical loads reveal an irreversible pile head displacement of approximately 0.1077 mm and almost 0 mm in the tests T_M1 and T_M2, respectively, corresponding to only 0.028 % (T_M1) and 0 % (T_M2) of the pile diameter, respectively. The application of monotonic and cyclic thermal loads to the pile between the two tests did not affect the pile-bearing capacity. This result aligns with the reported by Wang et al. [17], during monotonic heating, suggesting a thermoelastic response. While some others observed a decrease in shaft resistance [25,8,61,62]. Ren et al. [25] attributed the decrease in the pile capacity to the deformation at the interface and the changes in the thermophysical properties of the soil around the pile, leading to a decrease in pile capacity. In this study, the shaft had been densified during the pile installation. For this reason, almost no impact is seen, confirming the benefits of displacement cast in situ energy piles. Furthermore, the pore water viscosity in saturated soft soil may have contributed to the swift recovery of the pile-soil interface and thus no shaft degradation [63].

4.2. Thermo-mechanical behavior under thermal loads

4.2.1. Temperature variations

Fig. 3 shows the temperature variation versus elapsed time for the tests T_0 (Fig. 3(a)), T_20 (Fig. 3(b)), and T_60 (Fig. 3(c)).

The lowest temperature variation is noted in test T_0 with an average of 5 °C while in T_20, and T_60 an average of 10 and 11 °C can be observed respectively, noting that the minimum temperature of tests T_0 and T_20 remains above the freezing point (0 °C) along the pile, while in test T_60 the temperature drops below 0 °C. This may occur in practice due to the over-extraction of heat, failure of the system, or low initial ground temperature.

In test T_0, within the cooling phase, the temperature change in the upper (levels 1, 2 and 3) and lower part of the pile (levels 4, 5 and 6) were approximately 6 and 4 °C, respectively. After 38 days it reduced especially in the upper part, this is because of the influence of the ambient temperature on the upper part of the pile (see the air temperature in Fig. 10(a)) and thus on the energy demand. The average residual temperature at the end of this test, at level 1 was approximately 4 °C, while 2 °C at levels 2 and 3. However, in the lower part of the pile, (level 4–6) approximately −2 °C of low-residual temperature was observed.

In test T_20, the temperature change in the upper was approximately 11 °C except from level 2, where 8 °C was seen. This can be attributed to the low thermal conductivity of the peat. In the lower part of the pile, the temperature change was approximately 9 °C. The cooling target was nearly similar throughout this test, while during natural heating, the temperature was not fully recovered and tended to decrease due to the reduction in thermal energy in the soil surrounding the pile, leading to a residual temperature reduction of 4 °C at the end of this test.

In test T_60, the temperature change in the upper and lower part was approximately 11 and 9 °C, respectively. In this test, in the first 24 h of cooling the temperature was controlled to be above the freezing point, while in the second 24 h, the temperature was allowed to drop, representing an extreme scenario of GSHP operation. As seen in Fig. 3(c), the recorded temperature along the pile was approximately −1 °C.

Note that within the cooling phase, the variability exhibited can be seen due to the stoppage time of the GSHP in all conducted tests. The highest variability of 3 °C i.e., hourly/daily temperature fluctuation is seen in test T_0 when the GSHP operated naturally. This is because when the target temperature is reached, the GSHP stops automatically and when the temperature drops below the target, the GSHP starts again to maintain the temperature constant. A similar observation was reported by McCartney and Murphy [19]. While in the other tests, the observed variability was lower, about 1 °C.

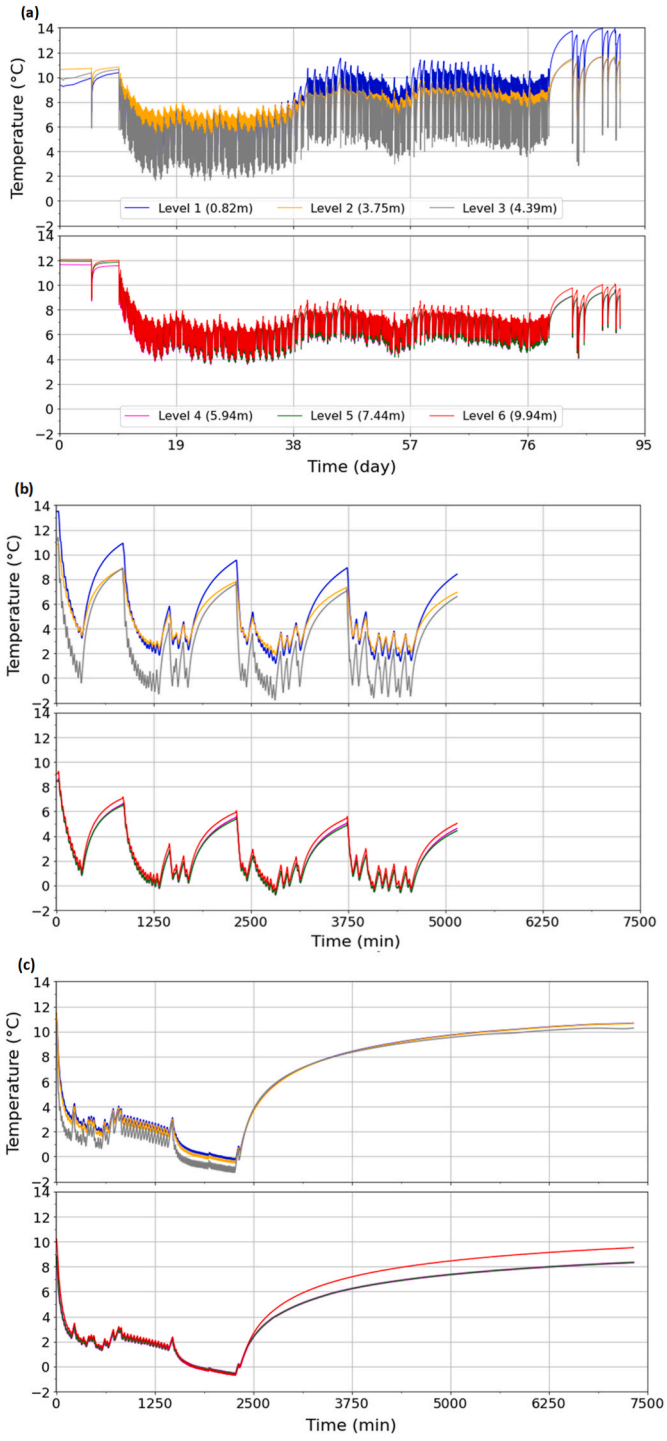

Fig. 3. Measured temperature change along the energy pile in the test: (a) T_0, (b) T_20, and (c) T_60.

4.2.2. Thermally induced strain

The (incremental) axial strains are shown in Fig. 4(a), (b), and (c) for

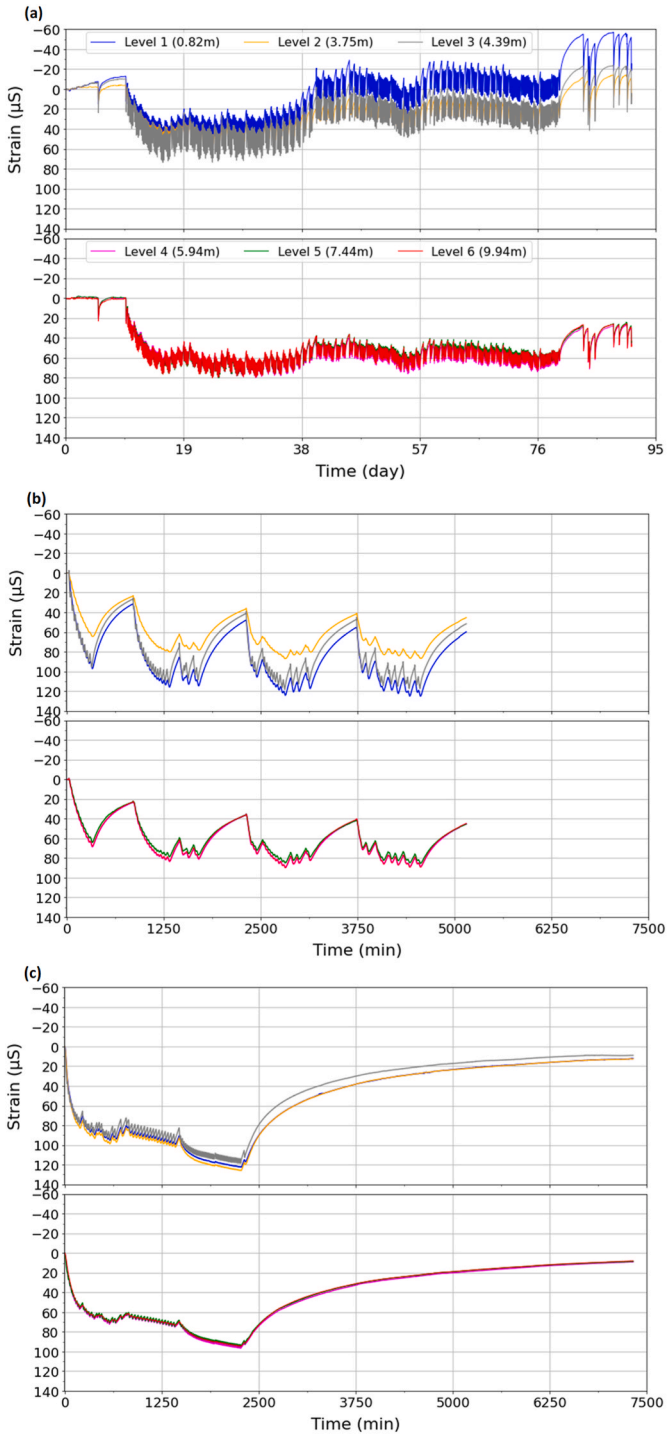

Fig. 4. Thermally induced strain increments variation of the pile versus elapsed time during thermal load of the test: (a) T_0, (b) T_20, and (c) T_60.

the tests T_0, T_20, and T_60, respectively, while their variations with temperature change are shown in Fig. 5(a), (b), and (c) for the tests T_0, T_20, and T_60 respectively.

As expected, contraction was observed during cooling, and during natural heating expansion reduced the net contraction or may even induce pure expansion when the temperature increases above its initial value. The thermal axial strain was observed to vary with depth in the foundation, depending on the temperature change and the restraint provided by the soils along the pile. In test T_0, the highest and the lowest thermally induced strains are observed in the upper part (levels 1, 2, and 3), and the lower part of the pile (levels 4, 5, and 6), respectively, following the temperature magnitude, being higher in the lower part.

In test T_20, in the upper part (first 3 levels), the highest strain was observed at level 1, even with lower temperature change compared to level 3 (see Fig. 5(b)). This confirms that the made ground is the weakest layer. Thus, less resistance, and high deformation (as seen in the mechanical results). While in the other levels, the strain seems to be driven mostly by temperature change and slightly affected by boundary conditions. With the increase in the number of temperature cycles during thermo-mechanical tests, the thermal strain curves manifested a downward trend, leading to a residual strain at the end of these tests. These residual strains could be largely due to the low residual temperature.

In test T_60, in the upper part, the lowest strain was observed at level 3 (similar to test T_20). This is because of the stronger restraint imposed by silty fine sand (level 3), where higher stress levels are expected (see Fig. 9). In the lower part, the results showed that the lowest strain was at level 6, while level 4 and 5, having the same deformation. This is because level 6 was in sandy soil which provides higher shaft resistance and thus lower deformation. However, levels 4 and 5 were in silty sand which provides nearly the same shaft resistance and thus identical deformations, despite the distance between these two levels. At the end of this test, residual strains are observed being lower compared to test T_20, due to the lower low-residual temperature. Across all gauges, some hysteresis is seen, with the lowest amount being observed in the free expansion test (T_0) at all levels. This is possibly due to the ratcheting effect under thermo-mechanical loads, i.e. the cumulative increases in displacement under repeating cycles. The higher the mechanical load, the higher the amount of hysteresis/ratcheting is observed. This phenomenon can be attributed to the stop/start operation of GSHP within cooling load (noted previously as variability in temperature) leading to a decrease/increase of thermally induced strain. Also, the incomplete pile and soil temperature recovery during natural heating, results in an increase in low-residual temperature over cycles in each test (see Fig. 3). Another possible reason for ratcheting could be the pile displacement relative to the adjacent soil. This phenomenon has been studied through laboratory tests on soil-structure interfaces by Golchin et al. [6] and Rafai et al. [7]. A shear displacement due to the thermal load in a ratcheting pattern was observed. In this test, the surrounding soils including the sand beneath the pile tip have been cooled over time, causing the ground to shrink. This shrinkage may induce a dragdown effect on the pile, leading to a temporary reduction of the pressure at the pile-soil interface, and thus further settlement. Further evidence of ratcheting effects can be seen in the results of pile head displacement. It should be not that, although the residual strains are small and appear to be related to the low-residual temperature, they might consist of the mechanical strain imposed by the dragdown of soils, as expensive/-contractive soft soils tend to deform plastically [42,45,623]. Moreover, Rafai et al. [56] reported that the higher the initial stress, the more susceptible soil is to thermally-induced contraction during cooling. This can also explain the ratcheting effects, especially under high mechanical load.

4.2.3. *Thermally induced stress*

The results of thermally induced stresses during thermal loading in all tests versus elapsed time are shown in Fig. 6(a), (b), and (c) for the energy foundation under 0 %, 20 %, and 60 % of the estimated bearing capacity, respectively, while their variations with temperature change are shown in Fig. 7(a), (b), and (c) for the tests T_0, T_20, and T_60 respectively. These results reflect the changes in axial stress within the pile due to the applied thermal load. It can be observed that cooling decreased the axial stress at all levels, indicating a tensile stress increment, and the latter increased during natural heating, resulting in a compressive stress increment. During the free expansion test (T_0), when the pile had the greatest freedom to deform, the lowest tensile stress was generated during cooling. Moreover, compressive and tensile stresses

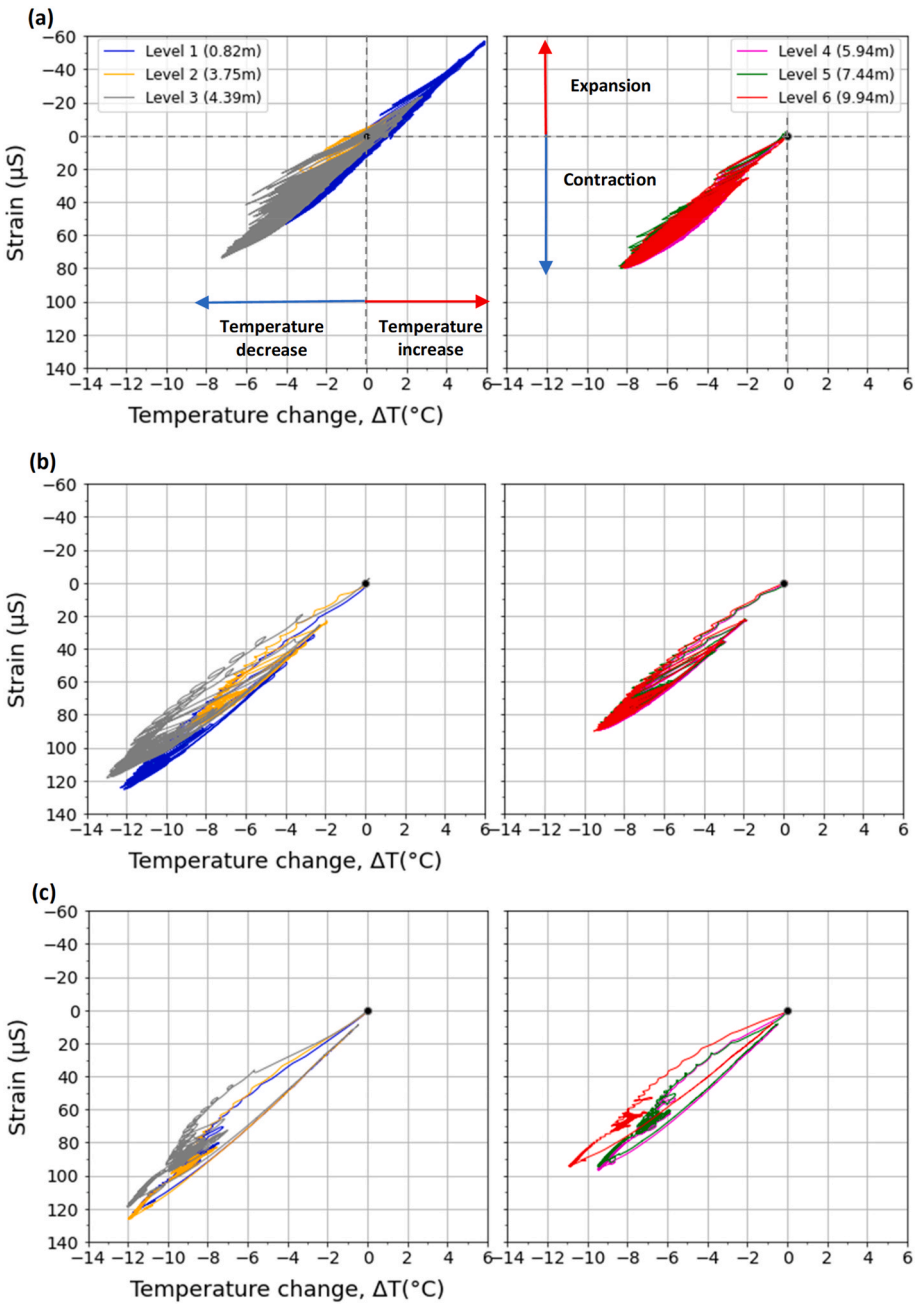

Fig. 5. Thermally induced strain increments variation of the pile versus temperature change during thermal load of the test: (a) T_0, (b) T_20, and (c) T_60.

are induced, indicating that such stresses may coexist within the same pile during a period of GSHP operation, leading to different trends of residual stress, i.e., tensile and compressive stresses in the first 4 and the last 2 levels respectively. This can be attributed to the heterogeneous nature of the temperature change along the pile, including the stoppage time of the GSHP along with the soil temperature change and thus strain/stress. When the pile was restrained by the applied mechanical loads (T_20 and T_60), the tensile stress increment was relatively higher under higher mechanical load during cooling (with respect to the temperature change), and subsequent natural heating led to a notable compressive stress along the pile shaft in those two tests.

When the cooling phase started (before transferring the cold load to the subsurface), maximum tensile stress was generated, which decreased over time during the cooling phase. This decrement was higher under a higher mechanical load. Similarly, the maximum compressive stress was generated during natural heating.

In test T_20, the tensile stress increments decreased with increasing the number of cycles. The stress change in the pile during cooling and natural heating cycles may include residual compressive stresses and thermally induced stresses, leading to a residual contractive stress at the end of these tests (i.e. a shift from tensile to contractive stress). The development of residual compressive stresses at the end of each cooling-natural heating cycle led to lower tensile stresses and higher compressive stresses during pile cooling and natural heating, respectively. This phenomenon can be explained by the combined effects of the dragdown of the surrounding soil due to the subsurface shrinkage during the cold load and the compression imposed on the pile head.

In test T_60, initially, the stress was higher and then started to decrease with time during phase 1. However, during phase 2, the stress remained constant, although the strain increased during this period (see Fig. 4(c)), following the increase in temperature reduction.

This is possibly because the rate of ground deformation significantly

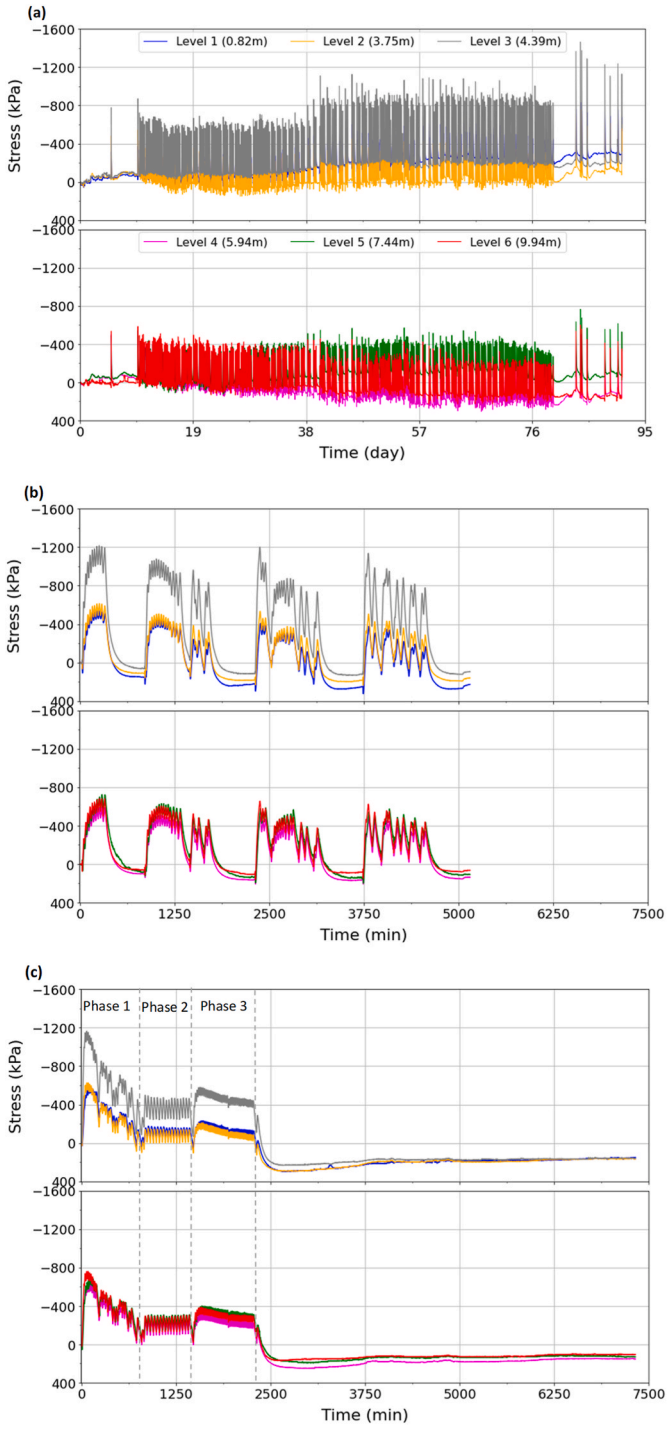

Fig. 6. Thermally induced stress increments variation of the pile versus elapsed time during thermal load of the test: (a) T_0, (b) T_20, and (c) T_60.

decreased, and it was almost stable during phase 2. During phase 3, (when the apparent freezing was seen) the stress started to reduce at a significantly slower rate compared to phase 1 but higher than phase 2. This can be explained either by, i) first, the ground had deformed previously, and its deformation rate reduces compared to the pile deformation with further cooling down the pile and soil, and/or ii) second, the pile interface was frozen during this phase. In this case, the interface would deform less compared to an unfrozen one, and thus less stress reduction.

As stated previously, the thermal creep at the pile interface as well as the dragdown of the surrounding soil could alleviate the tensile stress.

Similar to the thermal strain results, an important amount of hysteresis can be observed under higher mechanical load, probably due to the ratcheting effect combined with the dragdown of the subsurface. Further evidence is seen in the pile head displacement section.

It can be seen that the stress (at the first cycle, before its reduction) near the pile head strongly depends on the applied mechanical load and it is higher under higher applied mechanical load. However, further with depth, at other levels, the axial stress seems to be dominated and impacted by the temperature variation and slightly by the mechanical load. This is because the load was away from these levels compared to level 1 (where the load was immediately above this zone), indicating that at such zones shaft resistance plays a significant role in the thermally induced stresses. It is seen that within the same energy pile (see Fig. 6) non-uniform stresses were induced along the pile, depending on the restraining effect of the surrounding soils, and temperature change. This aligns with the numerical analyses performed by Abdelaziz and Ozudogru [64].

4.2.4. *Thermally induced mobilized shaft resistance*

The shaft friction resistance was calculated from the stresses shown in Fig. 6 and obtained from two adjacent layers of strain gauges. The variations in mobilized shaft resistance for each zone (as delineated in Fig. 2(b)) along the pile versus elapsed time during thermal load of the three tests, T_0, T_20, and T_60 are shown in Fig. 8(a), (b), and (c) respectively, while their variations with temperature change are shown in Fig. 9(a), (b), and (c) respectively.

In zone A, near the pile head, observations from Figs. 8 and 9 suggest that at the initial cooling phase, the mobilized shaft friction appeared to be higher under higher mechanical load. Subsequent cooling led to a drastic decrement in the upward friction, especially under higher mechanical load. For example, in test T_20 the initial shear stress that was generated at the first moments of cooling was approximately 70 kPa while in test T_60 was 80 kPa. Moreover, during the first moment of natural heating cycle, the shear stresses were approximately −35 and −42 kPa in tests T_20 and T_60 respectively. At the end of these two tests, negative shear stress is observed at this zone. This is maybe because the applied mechanical load was immediately above this zone, which restrains the possible deformation leading to residual shear stress. However, in test T_0, no negative shear stress is seen in zone A. This is likely because at this zone, the pile during natural heating the pile expanded freely (upward), and as made ground layer provides almost no restrains effect (maximum expansion seen, see Fig. 4), thus, no negative shear stress is noted. While the observed positive shear stress in this zone can be explained by the fact that the pile deforms towards the null point. Therefore, the expected uplift of the lower part of the pile can induce restraining effects on zone A, and thus positive shear stress would be generated. A similar trend can be seen in zone C of these tests, while the opposite was observed in zone D. In zone F, clear negative friction can be observed. Additionally, residual negative shear stress was noted at the end of this test (T_0), possibly due to the unrecovered temperature along with the potential successive dragdown of the near soils. This aligns with the residual compressive strain previously. However, when the pile was under mechanical load, in zone F, initially positive friction was evident, possibly due to a larger settlement along the pile.

During cooling load, and under higher mechanical load, a switch from positive to negative friction was observed in zone F, due to the pile's additional shrinkage coinciding with soil contraction as a result of the cold load. It should be noted that higher positive friction was observed in zone C compared to zone A, while the strain results revealed the opposite (higher contraction at level 1 compared to level 3) due to the higher resistance imposed by the silty sand layer compared to the made ground layer. In the three conducted tests, the lowest shear stress (nearly zero) was observed at zone B; maybe due to the low resistance combined with soil deformation.

In thermo-mechanical tests, the shear stress appears to be higher in test T_20 in zones C and D compared to test T_60. This is possibly

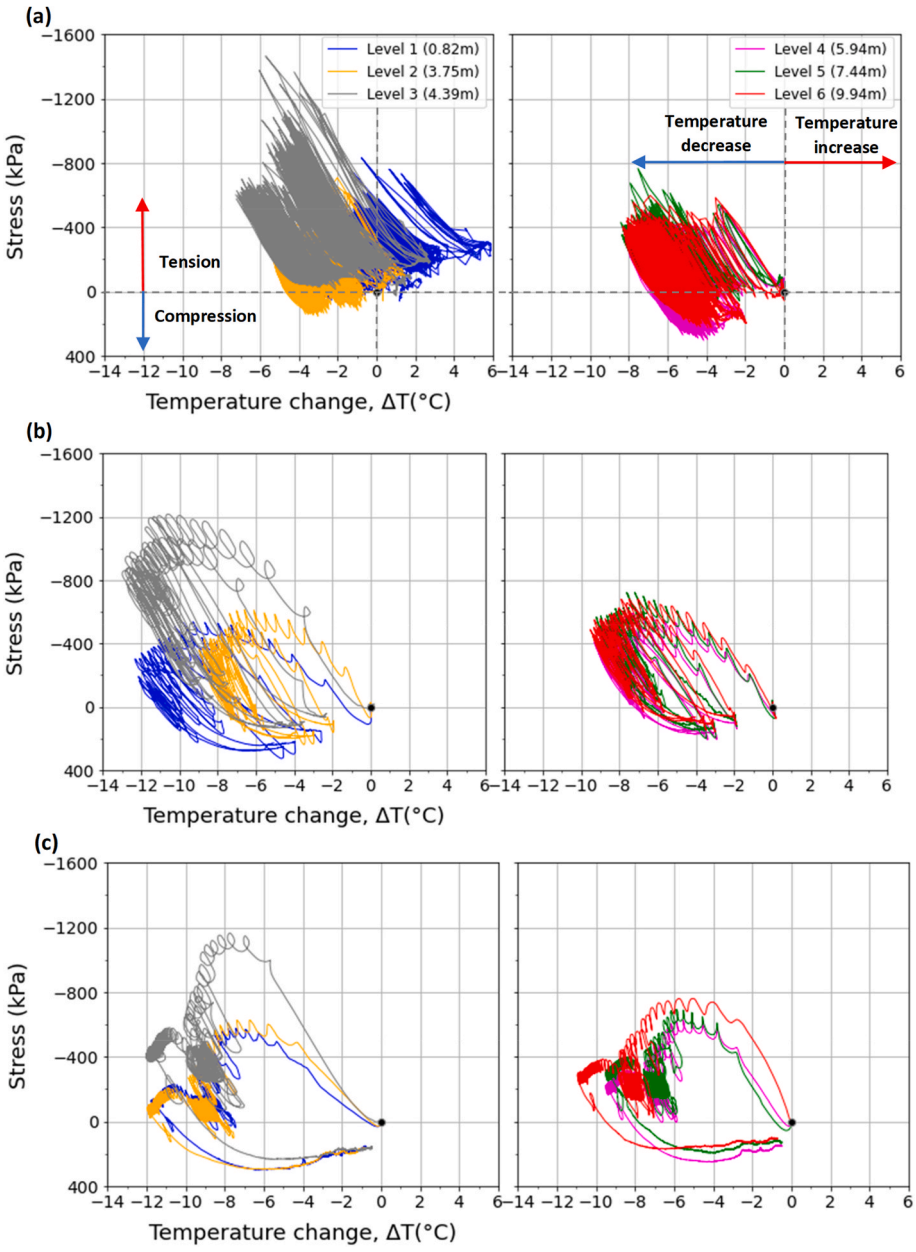

Fig. 7. Thermally induced stress increments variation of the pile versus temperature change during thermal load of the test: (a) T_0, (b) T_20, and (c) T_60.

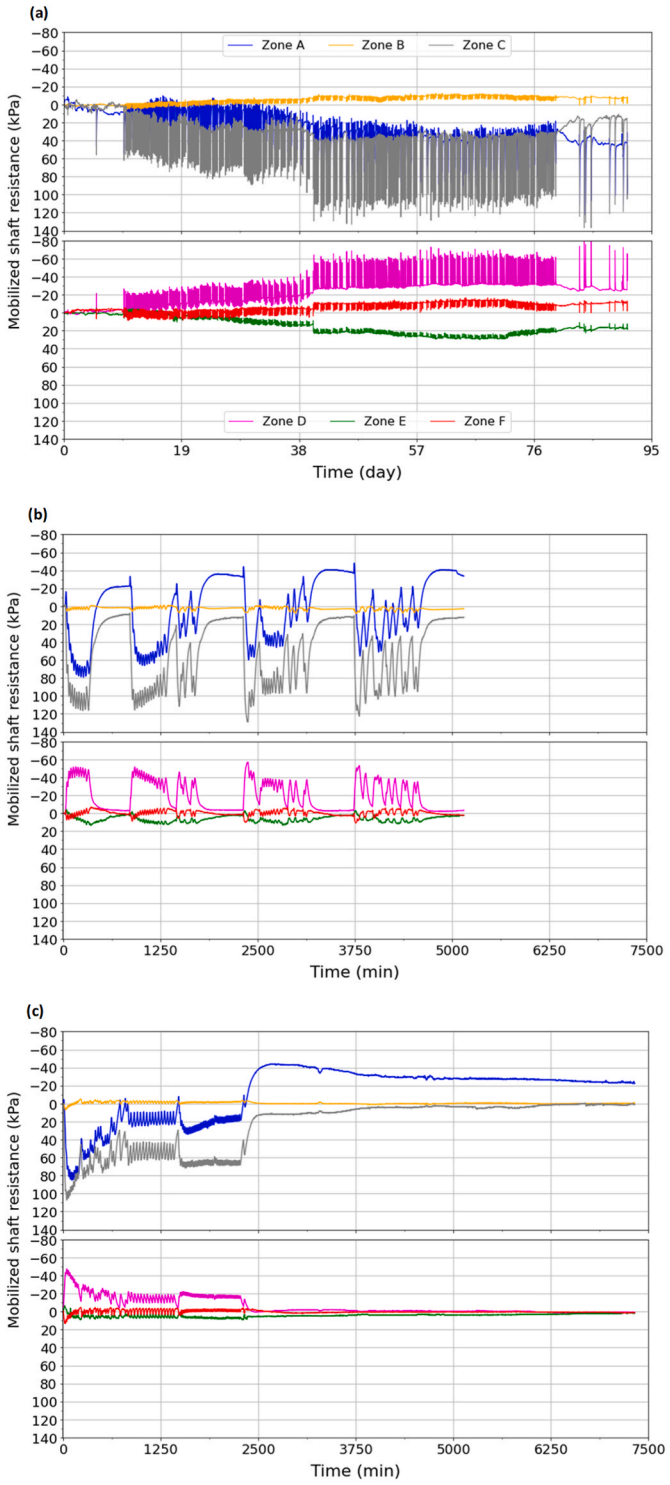

Fig. 8. Mobilized shaft resistance variation of the pile versus elapsed time during thermal load of the test: (a) T_0, (b) T_20, and (c) T_60.

because of the higher contraction/expansion magnitude during cooling/natural-heating under lower mechanical load compared to higher mechanical load due to higher temperature change and low-restraining effects as the impact of the applied mechanical load reduces with depth.

4.2.5. *Thermally induced pile head displacements*

Pile head displacements, along with the air and the pile temperature measured by the LVDT and gauges at level 1, versus elapsed time, are shown in Fig. 10(a), (b), and (c) for tests T_0, T_20, and T_60, respectively, during the thermal load. These figures reflect the changes in pile head displacement due to the applied thermal load. In Fig. 11(a), (b), and (c) the pile head displacement is plotted versus the pile temperature change during the cooling–natural heating loads for tests T_0, T_20, and T_60, respectively. These figures (Figs. 10 and 11) illustrate the pile thermal behavior under different degrees of freedom. During the first cooling phase (when temperature decreased), the pile settled in all tests. The subsequent natural increase in pile temperature during natural heating caused an uplift in all tests. In the free expansion test (T_0), the results reveal a large pile head uplift during natural heating, leading to an irreversible pile head uplift of 0.2 mm. This is likely due to the high-residual temperature of 4 °C at the upper part of the pile which is consistent with the residual expansive strains in the upper part of the pile, along with the impact of the previous testing program which had caused residual contractive strains and irreversible settlement [3]. In thermo-mechanical tests (T_20, and T_60), similarly, the pile head settled during the first cooling phase, with higher settlements observed under higher mechanical load with respect to the temperature variation. The subsequent natural increase in pile temperature during natural heating led to uplift but it did not fully recover, i.e. permanent settlement was observed. This implies an accelerated ratcheting effect at the pile-soil interface rather than expansion and contraction of the pile due to the temperature change. The pile head uplift during natural heating is dependent on the applied mechanical load and is lower under higher mechanical load. This trend was consistent throughout test T_20 but at a small rate, following the magnitude of temperature change. At the end of this test, after four thermal cycles, a settlement of 0.15 mm is observed, with −4 C° of low-residual temperature. In test T_60, after one thermal cycle 0.17 mm is noted, with less than −1 C° of low-residual temperature. This is higher than the observed in test T_20, even though the residual temperature was lower, indicating a major impact of thermal load on the pile head displacement. Since low pile head displacement was observed in test T_20 and higher unrecovered temperature, the plastic deformation is largely due to the residual low-temperature. The higher displacement in test T_60 could be mostly due to the thermal ratcheting at the soil-structure interface (seen previously as hysteresis, see Fig. 7) [6,7,56] and the contraction of the surrounding soil including the sand beneath the pile tip [55,56]. The shrinkage of the surrounding soil was clearly manifested as a significant reduction in the generated stress (see Fig. 6(c)). The observed irreversible pile head displacement in the present study is consistent with previous findings on the pile head settlement with thermal cycles [24–26,28,29], and also, at the soil-structure interface [6,7,56]. Nguyen et al. [38] reported that the irreversible settlement continued to increase after 20 cycles only when the pile head load was high. This behavior is particularly critical in the case of floating energy piles, where irreversible ratcheting settlement of elevated pile groups exceeded serviceability and ultimate criteria [8]. They attribute this behavior to a decrease in the resistance of the pile-soil interface with an increasing number of thermal cycles. However, in this study, such effects remained limited. Kong et al. [65] reported that the reduction in shaft resistance contributes to pile settlement. This reduction in shaft resistance piles was attributed to the thermally induced settlement of the sandy soil surrounding the piles. The thermal settlement of the soil decreased the relative displacement of the piles with respect to the surrounding soil and thus led to the reduction of shaft resistance [30]. Although indications of the subsurface dragdown were noted in this study, its impact on shaft reduction is likely to be temporary as almost no impact of thermal loads on shaft resistance was observed (see Fig. 2). Fang et al. [28] observed that the pile head displacement evolved in a ratcheting pattern due to the thermo-mechanical loads. The study on thermally induced soil-structure displacement by Rafai et al. [56] reveals irreversible lateral settlements (i.e., shear displacement) evolving in a ratcheting pattern due to the imposed thermo-mechanical load. These settlements ranged from 0.08 to 0.38 mm after 20 thermal cycles depending on the soil density and the applied normal stress [56]. The observed irreversible pile head displacement of 0.17 mm falls within this

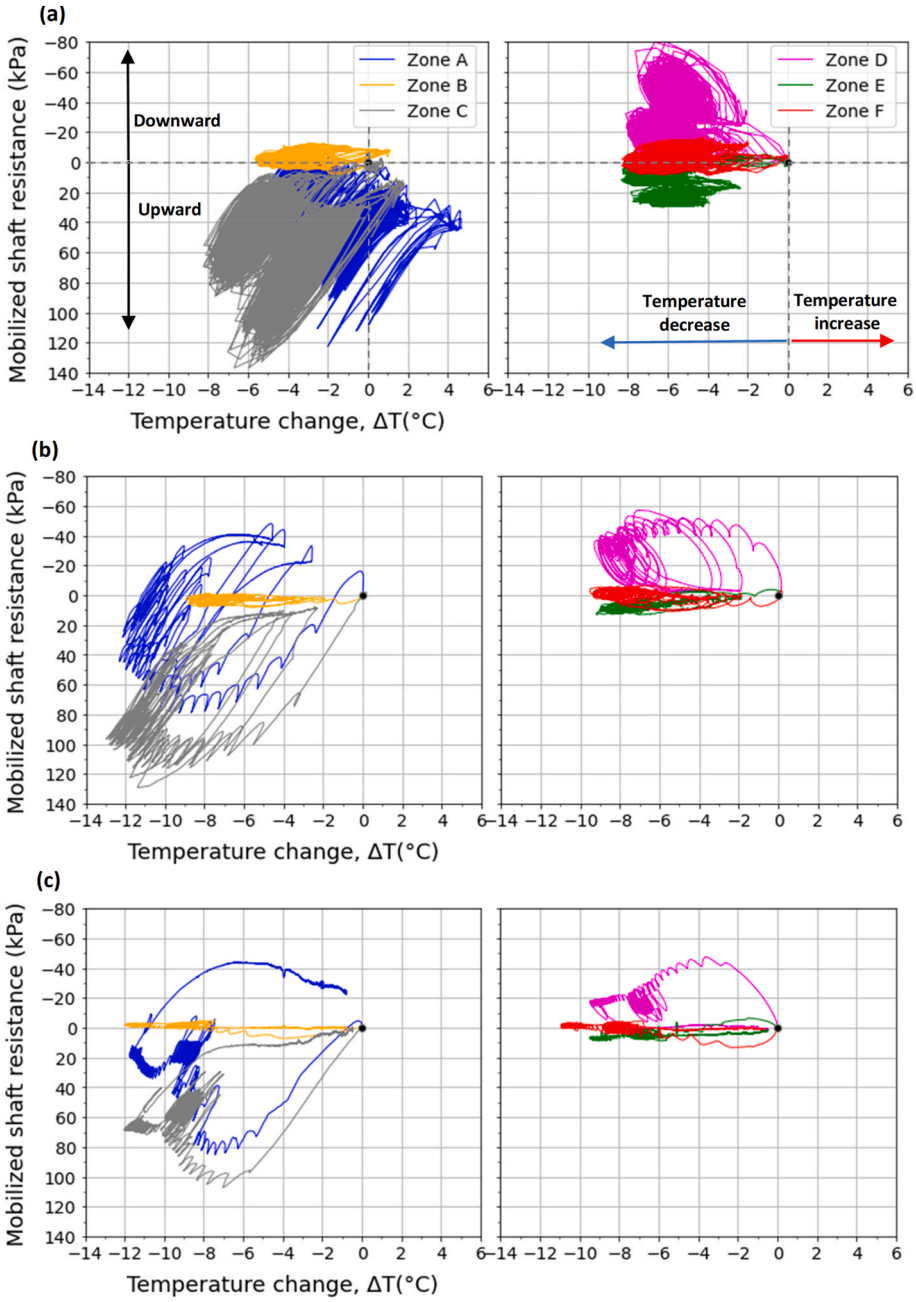

Fig. 9. Mobilized shaft resistance variation of the pile versus temperature change during thermal load of the test: (a) T_0, (b) T_20, and (c) T_60.

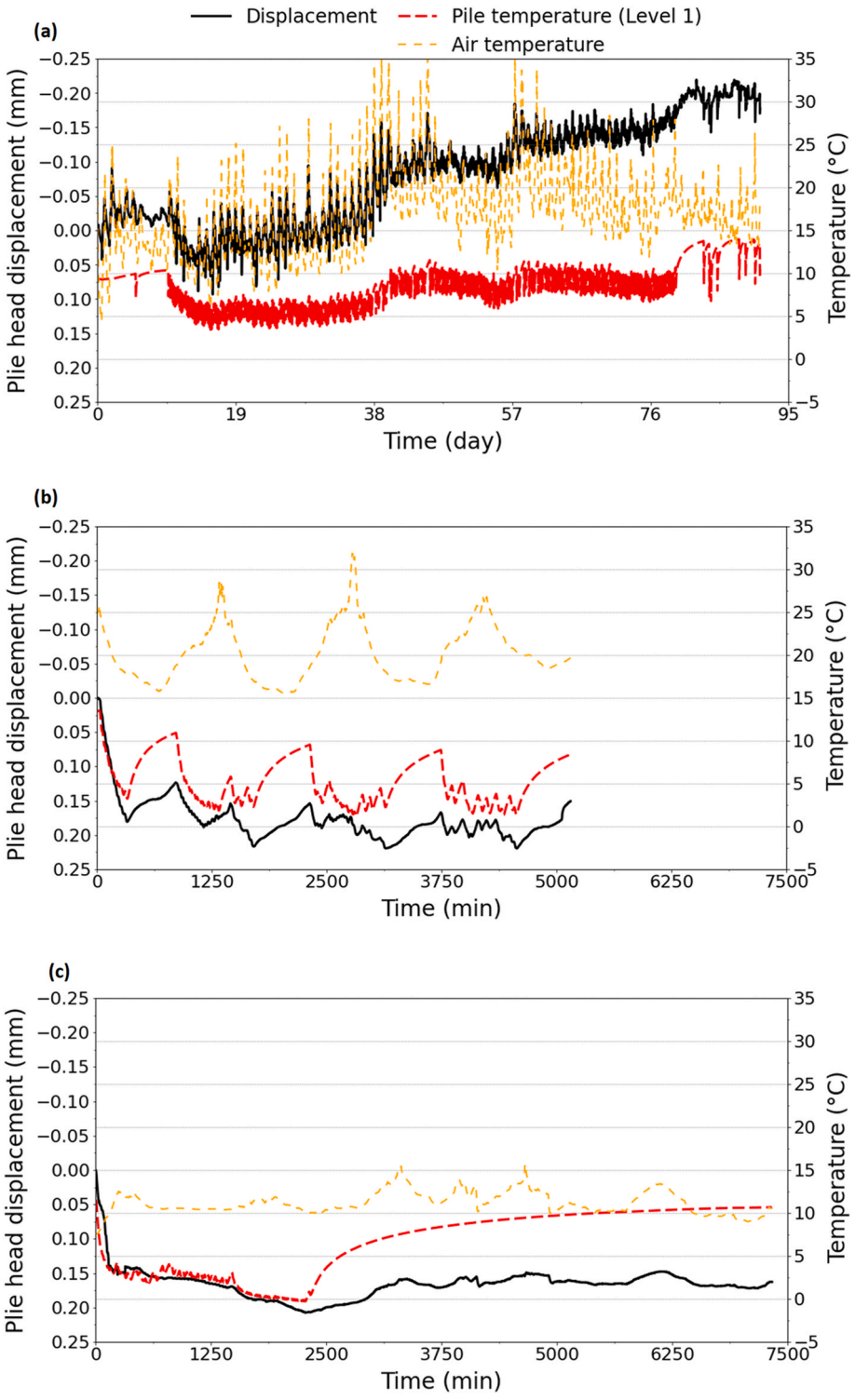

Fig. 10. Pile head displacement, air, and pile temperature variation (measured at the top of the pile) versus elapsed time of tests: (a) T_0, (b) T_20, and (c) T_60.

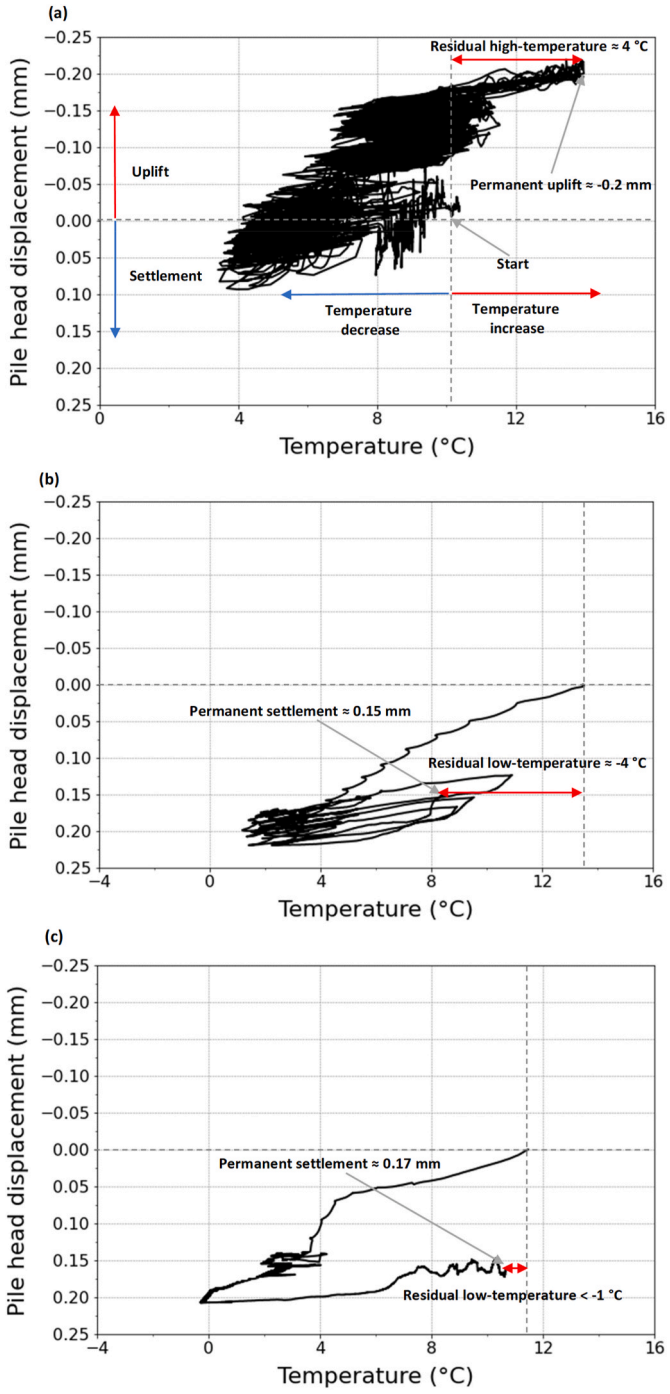

Fig. 11. Pile head displacement versus pile temperature of tests: (a) T_0, (b) T_20, and (c) T_60.

range and is acceptable in engineering practices, indicating that the freezing did not significantly contribute to the settlement, likely due to the densification of the ground as a result of the pile installation and dragdown effects during previous thermal cycles [3] or the pile-soil interface was not completely frozen. Rafai et al. [56] explained that the observed thermally induced shear displacement may be attributed to the coupled effect of the initial shear stress, which renders the soil-structure interface more susceptible to thermally-induced shear displacements. Consequently, thermal cycles modify the stress state at this zone due to the expansion and contraction of the grains during heating and cooling, leading to their rearrangements. The temporary decrease in the resistance of the soil–structure interface with an increasing number of thermal cycles further contributes to the ratcheting. This can explain the observed irreversible pile head displacement in test T_60. In addition, the contraction of sand beneath the pile tip under higher mechanical load would be more pronounced, as it is more susceptible to thermally induced perturbation compared to lower mechanical load [56]. This results in slippage and rearrangements, and therefore, more plastic deformation under higher normal stress compared to the pile under lower mechanical load, where the normal stress is minor. Further details are provided by Rafai et al. [56].

Thermo-mechanical creep, varying degrees of shrinkage at the soil-structure interface, and the sand beneath the pile tip could induce different magnitudes of strains, stresses, mobilized shaft friction, and pile head displacement. While this effect was insignificant in a semi-floating energy pile when high shaft and tip resistances could be involved, it should be considered in floating energy piles installed in very soft soil layers that could experience high magnitudes of dragdown and ratcheting.

5. Conclusions

In this study, thermally induced strains, stresses, and pile head displacements of a semi-floating displacement cast-in-situ energy pile in multilayered soft soils were investigated under the effects of long-term cooling (three months) and different constant applied mechanical loads (20, and 60 % of the pile capacity). The tests were conducted through full-scale in situ experiments, in Delft, The Netherlands. The field results confirm that the incorporation of ground-source heat exchange technology into displacement cast in-situ piles can provide sustainable heat exchange with no major effects on the structural performance of the building. The conclusions that can be drawn from the data analysis include:

- Under zero mechanical load, thermal load induced residual compressive and expansive strain/stress along the pile. Additionally, a 0.2 mm of permanent pile head uplift was observed at the end of this test.
- Under low constant mechanical load (20 % of the pile capacity), thermal cycles induced an irreversible compressive strain/stress and pile head settlement of 0.15 mm, attributed mainly to the accumulation of unrecovered temperature. Therefore, at such loading level, thermoelastic behavior was observed.
- Under high constant mechanical load (60 % of the pile bearing capacity) and extreme temperatures, compressive strain/stress, and higher but limited irreversible pile head displacement i.e., 0.17 mm, were observed. This was due to the larger contraction of sand beneath the pile tip and the thermal ratcheting of the soil-structure interface.
- Thermally induced strains and stresses and pile displacement in these conditions were within acceptable limits for typical engineering structures, including after interface freezing.
- Negligible impact of thermal load on the shaft and the overall pile capacity was observed. This was mainly attributed to the high shaft resistance of the pile as a consequence of its densification during the pile installation.

These findings provide valuable insights for the designing of thermo-active semi-floating energy piles in soft soils subjected to both monotonic and cyclic thermal loads under varying mechanical loads. However, the reported results are primarily applicable to heating-dominant climate. In scenarios with balanced heating-cooling demands, characterized by higher magnitude thermal cycles, or under higher applied mechanical loads, the thermal and structural behavior of energy piles may differ and could exhibit more critical response than those observed in this study. These aspects warrant further investigation to ensure comprehensive design consideration.

CRediT authorship contribution statement

Mouadh Rafai: Writing – review & editing, Writing – original draft, Visualization, Validation, Software, Methodology, Investigation, Funding acquisition, Formal analysis, Data curation, Conceptualization. **Diana Salciarini:** Writing – review & editing, Supervision, Funding acquisition. **Philip J. Vardon:** Writing – review & editing, Supervision, Funding acquisition.

Declaration of competing interest

The authors declare that they have no known competing financial interests or personal relationships that could have appeared to influence the work reported in this paper.

Acknowledgments

Part of the work presented was carried out within the scope of the following projects: Netherlands Organisation for Scientific Research (NWO) project number 14698 “Energy Piles in the Netherlands”; COST Action CA21156 “European network for FOstering Large-scale ImplementAtion of energy Geostructure (FOLIAGE)”; PRIN2022 “Closing knowledge gaps on energy geostructures for retrofitting of buildings and infrastructures (GEOREFIT)”; CETP22FP-2022-00147 “Large-scale climate neutral Energy Geostructures in District Heating & Cooling systems/networks (LEG-DHC)”; National Innovation Ecosystem grant ECS00000041 - VITALITY - CUP J97G22000170005. The first author appreciates ERASMUS + support.

References

[1] M. Tunzi, D.S. Østergaard, S. Svendsen, R. Boukhanouf, E. Cooper, Method to investigate and plan the application of low temperature district heating to existing hydraulic radiator systems in existing buildings, Energy 113 (2016) 413–421, https://doi.org/10.1016/j.energy.2016.07.033.
[2] M.I. Gida, District energy in Iceland, Tech. rep., Icelandic Energy & Utilities (2019).
[3] M. Rafai, D. Salciarini, P.J. Vardon, Full-scale in-situ tests on a displacement cast in situ energy pile: effects of cyclic thermal loads under different mechanical load levels on pile stress and strain, Geomech. Energy Environ. 40 (2024) 100606, https://doi.org/10.1016/j.gete.2024.100606.
[4] S.S. Meibodi, F. Loveridge, The future role of energy geostructures in fifth generation district heating and cooling networks, Energy 240 (2022) 122481, https://doi.org/10.1016/j.energy.2021.122481.
[5] L. Laloui, A.F.R. Loria, Analysis and Design of Energy Geostructures: Theoretical Essentials and Practical Application, Academic Press, 2019.
[6] A. Golchin, Y. Guo, P.J. Vardon, S. Liu, G. Zhang, M.A. Hicks, Shear creep behaviour of soil-structure interfaces under thermal cyclic loading, Géotech. Lett. 13 (1) (2023) 22–28, https://doi.org/10.1680/jgele.22.00009.
[7] M. Rafai, A. Minh Tang, T. Badinier, D. Salciarini, J. de Sauvage, Thermally induced shear displacement of sand-concrete interface under different stress levels, Symposium on Energy Geotechnics 2023 (2023), https://doi.org/10.59490/seg.2023.541.
[8] C.W. Ng, A. Farivar, S.M. Gomaa, F. Jafarzadeh, Centrifuge modeling of cyclic nonsymmetrical thermally loaded energy pile groups in clay, J. Geotech. Geoenviron. Eng. 147 (12) (2021) 04021146, https://doi.org/10.1061/(ASCE)GT.1943-5606.0002689.
[9] R. Zhao, A.K. Leung, J.A. Knappett, Thermally induced ratcheting of a thermo-active reinforced concrete pile in sand under sustained lateral load, Geotechnique 73 (9) (2022) 826–839, https://doi.org/10.1680/jgeot.21.00299.
[10] H. Brandl, Energy foundations and other thermo-active ground structures, Geotechnique 56 (2) (2006) 81–122, https://doi.org/10.1680/geot.2006.56.2.81.
[11] N. Batini, A.F. Rotta Loria, P. Conti, D. Testi, W. Grassi, L. Laloui, Energy and geotechnical behaviour of energy piles for different design solutions, Appl. Therm. Eng. 85 (2015) 199–213, https://doi.org/10.1016/j.applthermaleng.2015.04.050.
[12] F. Ronchi, D. Salciarini, N. Cavalagli, C. Tamagnini, Thermal response prediction of a prototype Energy Micro-Pile, Geomech. Energy Environ. 16 (2018) 64–82, https://doi.org/10.1016/j.gete.2018.07.001.
[13] P. Bourne-Webb, B. Amatya, K. Soga, P. Payne, Energy pile test at Lambeth College, London: geotechnical and thermodynamic aspects of pile response to heat cycles, Geotechnique 59 (3) (2009) 237–248, https://doi.org/10.1680/geot.2009.59.3.237.
[14] L. Laloui, M. Nuth, L. Vulliet, Experimental and numerical investigations of the behaviour of a heat exchanger pile, Int. J. Numer. Anal. Methods GeoMech. 30 (8) (2006) 763–781, https://doi.org/10.1016/B978-0-08-100191-2.00016-2.
[15] J.S. McCartney, K.D. Murphy, Strain distributions in full-scale energy foundations, DFI J. J. Deep Found. Inst. 6 (2) (2012) 26–38, https://doi.org/10.1179/dfi.2012.008.
[16] K.D. Murphy, J.S. McCartney, K.S. Henry, Evaluation of thermo-mechanical and thermal behavior of full-scale energy foundations, Acta Geotech 10 (2) (2015) 179–195, https://doi.org/10.1007/s11440-013-0298-4.
[17] B. Wang, A. Bouazza, R. Singh, C. Haberfield, D. Barry-Macaulay, S. Baycan, Posttemperature effects on shaft capacity of a full-scale geothermal energy pile, J. Geotech. Geoenviron. Eng. 141 (4) (2015) 04014125, https://doi.org/10.1061/(ASCE)GT.1943-5606.0001266.
[18] C. De Santiago, F.P. de Santayana, M. De Groot, J. Urchueguía, B. Badenes, T. Magraner, J. Arcos, F. Martín, Thermo-mechanical behavior of a thermo-active precast pile, Bulg. Chem. Commun. 48 (2016) 41–54.
[19] J.S. McCartney, K.D. Murphy, Investigation of potential dragdown/uplift effects on energy piles, Geomech Energy Environ 10 (2017) 21–28, https://doi.org/10.1016/j.gete.2017.03.001.
[20] M. Sutman, T. Brettmann, C.G. Olgun, Full-scale in-situ tests on energy piles: head and base-restraining effects on the structural behaviour of three energy piles, Geomech Energy Environ 18 (2019) 56–68, https://doi.org/10.1016/j.gete.2018.08.002.
[21] M. Faizal, A. Bouazza, C. Haberfield, J.S. McCartney, Axial and radial thermal responses of a field scale energy pile under monotonic and cyclic temperatures, J. Geotech. Geoenviron. Eng. 144 (10) (2018) 04018072, https://doi.org/10.1061/(ASCE)GT.1943-5606.000195.
[22] M. Faizal, A. Bouazza, J.S. McCartney, C. Haberfield, Axial and radial thermal responses of an energy pile under a 6-storey residential building, Can. Geotech. J. 56 (2018) 1019–1033, https://doi.org/10.1139/cgj-2018-0246.
[23] M. Faizal, A. Bouazza, J.S. McCartney, C. Haberfield, Effects of cyclic temperature variations on thermal response of an energy pile under a residential building, J. Geotech. Geoenviron. Eng. 145 (10) (2019) 04019066, https://doi.org/10.1061/(ASCE)GT.1943-5606.000214.
[24] G. Jiang, C. Lin, D. Shao, M. Huang, H. Lu, G. Chen, C. Zong, Thermo-mechanical behavior of driven energy piles from full-scale load tests, Energy Build. 233 (2021) 110668, https://doi.org/10.1016/j.enbuild.2020.110668.
[25] L.-w. Ren, J.-y. Ren, Z.-p. Han, J. Xu, Field tests on the thermomechanical responses of PHC energy piles under cooling and loading conditions, Acta Geotech 18 (2023) 429–444, https://doi.org/10.1007/s11440-022-01559-9.
[26] G. Kong, R. Li, H. Deng, Q. Yang, Behaviours of a belled energy pile under heating-cooling cycles, J. Build. Eng. 72 (2023) 106652, https://doi.org/10.1016/j.jobe.2023.106652.
[27] M. Rafai, D. Salciarini, P.J. Vardon, Thermo-mechanical response of a cast in situ displacement energy pile, EGU General Assembly (2024), https://doi.org/10.5194/egusphere-egu24-7965. Vienna, Austria, 14–19 Apr 2024, EGU24-7965, 743.
[28] J. Fang, G. Kong, Q. Yang, Group performance of energy piles under cyclic and variable thermal loading, J. Geotech. Geoenviron. Eng. 148 (8) (2022) 04022060, https://doi.org/10.1061/(ASCE)GT.1943-5606.0002840.
[29] G. Jiang, D. Shao, C. Zong, G. Chen, J. Huang, C. Lin, X. Wang, Y. Zhang, Thermo-mechanical behavior of long-bored energy pile: a full-scale field investigation, KSCE J. Civ. Eng. 27 (1) (2023) 145–155, https://doi.org/10.1007/s12205-022-0588-1.
[30] M. Rafai, D. Salciarini, P.J. Vardon, Energy pile displacements due to cyclic thermal loading at different mechanical load levels, Acta Geotech (2025). https://doi.org/10.1007/s11440-025-02556-4.
[31] M.A. Stewart, J.S. McCartney, Centrifuge modeling of soil–structure interaction in energy foundations, ASCE J Geotech. Geoenviron. Eng 140 (4) (2014) 04013044, https://doi.org/10.1061/(ASCE)GT.1943-5606.0001061.
[32] N. Yavari, A.M. Tang, J.-M. Pereira, G. Hassen, Experimental study on the mechanical behaviour of a heat exchanger pile using physical modelling, Acta Geotech 9 (3) (2014) 385–398, https://doi.org/10.1007/s11440-014-0310-7.
[33] J.C. Goode III, J.S. McCartney, Centrifuge modeling of end-restraint effects in energy foundations, J. Geotech. Geoenviron. Eng. 141 (8) (2015) 04015034, https://doi.org/10.1061/(ASCE)GT.1943-5606.0001333.
[34] J.C. Goode III, M. Zhang, J.S. McCartney, Centrifuge modeling of energy foundations in sand, in: C. Gaudin, D. White (Eds.), Physical Modeling in Geotechnics: Proc. 8th International Conference on Physical Modelling in Geotechnics. Perth, Australia. Jan. 14-17, Taylor and Francis, London, 2014, pp. 729–736.
[35] J.C. Goode III, J.S. McCartney, Evaluation of head restraint effects on energy foundations, in: M. Abu-Farsakh, L. Hoyos (Eds.), Proc. GeoCongress 2014, GSP 234, ASCE, 2014, pp. 2685–2694.
[36] C.W.W. Ng, A. Gunawan, C. Shi, Q.J. Ma, H.L. Liu, Centrifuge modelling of displacement and replacement energy piles constructed in saturated sand: a comparative study, Géotech. Lett. 6 (1) (2016) 34–38, https://doi.org/10.1680/jgele.15.00119.
[37] N. Yavari, A.M. Tang, J.-M. Pereira, G. Hassen, Mechanical behaviour of a small-scale energy pile in saturated clay, Geotechnique 66 (11) (2016) 878–888, https://doi.org/10.1680/jgeot.15.T.026.
[38] V.T. Nguyen, A.M. Tang, J.-M. Pereira, Long-term thermo-mechanical behavior of energy pile in dry sand, Acta Geotech 12 (4) (2017) 729–737, https://doi.org/10.1007/s11440-017-0539-z.
[39] A. Vieira, J. Maranha, Thermoplastic analysis of a thermoactive pile in a normally consolidated clay, Int. J. GeoMech. 17 (1) (2017) 04016030, https://doi.org/10.1061/(ASCE)GM.1943-5622.0000666.
[40] S. Yazdani, S. Helwany, G. Olgun, Investigation of thermal loading effects on shaft resistance of energy pile using laboratory-scale model, J. Geotech. Geoenviron.

Eng. 145 (9) (2019) 04019043, https://doi.org/10.1061/(ASCE)GT.1943-5606.0002088.
[41] Y. Rui, M. Yin, Investigations of pile–soil interaction under thermomechanical loading, Can. Geotech. J. 55 (7) (2018) 1016–1028, https://doi.org/10.1139/cgj-2017-0091.
[42] D. Wu, H. Liu, G. Kong, C. Li, Thermo-mechanical behavior of energy pile under different climatic conditions, Acta Geotech 14 (2019) 1495–1508, https://doi.org/10.1007/s11440-018-0731-9.
[43] A. Lupattelli, D. Salciarini, F. Cecinato, M. Veveakis, T.M. Bodas Freitas, P. J. Bourne-Webb, Temperature dependence of soil-structure interface behaviour in the context of thermally-activated piles: a review, Geomech. Energy Environ. 37 (2024) 100521, https://doi.org/10.1016/j.gete.2023.100521.
[44] A.F. Rotta Loria, A. Gunawan, C. Shi, L. Laloui, C.W.W. Ng, Numerical modelling of energy piles in saturated sand subjected to thermomechanical loads, Geomech Energy Environ 1 (2015) 1–15, https://doi.org/10.1016/j.gete.2015.03.002.
[45] D.M. Chen, Soil Structure Interaction in Energy Piles Master Thesis, Structural Engineering, University of California, San Diego, San Diego, CA, 2016.
[46] K.A. Gawecka, D.M.G. Taborda, Numerical modelling of thermo-active piles in London Clay, Geotech. Eng. 170 (2017) 201–219, https://doi.org/10.1680/jgeen.16.00096.
[47] C. Knellwolf, H. Peron, L. Laloui, Geotechnical analysis of heat exchanger piles, J. Geotech. Geoenviron. Eng. 137 (10) (2011) 890–902, https://doi.org/10.1061/(ASCE)GT.1943-5606.00005.
[48] D. Salciarini, F. Ronchi, C. Tamagnini, Thermo-hydro-mechanical response of a large piled raft equipped with energy piles: a parametric study, Acta Geotech 12 (2017) 703–728, https://doi.org/10.1007/s11440-017-0551-3.
[49] M. Rafai, A. Lupattelli, D. Salciarini, Finite element modelling of energy piles using different constitutive models for the soil, XI Incontro Annuale dei Giovani Ingegneri Geotecnici, IAGIG 2022 (2022) 83–86.
[50] C.W. Ng, X. Zhao, S. Zhang, J. Ni, C. Zhou, An elasto-plastic numerical analysis of THM responses of floating energy pile foundations subjected to asymmetrical thermal cycles, Geotechnique 74 (7) (2022) 600–619, https://doi.org/10.1680/jgeot.22.00055.
[51] P.J. Bourne-Webb, A. Lupattelli, T.M.B. Freitas, D. Salciarini, The influence of initial shaft resistance mobilisation in the response of seasonally, thermally-activated pile foundations in granular media, Geomech Energy Environ 32 (2022) 100299, https://doi.org/10.1016/j.gete.2021.100299.
[52] R. Caulk, E. Ghazanfari, J.S. McCartney, Parameterization of a calibrated geothermal energy pile model, Geomech Energy Environ 5 (3) (2016) 1–15, https://doi.org/10.1016/j.gete.2015.11.001.
[53] A. Lupattelli, P.J. Bourne-Webb, T.M. Bodas Freitas, D. Salciarini, A numerical study of the behavior of micropile foundations under cyclic thermal loading, Appl. Sci. 13 (17) (2023) 9791, https://doi.org/10.3390/app13179791.
[54] A. Lupattelli, D. Salciarini, Investigating the impact of temperature recovery across different thermal activation scenarios of a real-world energy piled foundation, Tunnell. Undergr. Space Technol. 158 (2025) 106457.
[55] J. Sittidumrong, A. Jotisankasa, K. Chantawarangul, Effect of thermal cycles on volumetric behaviour of Bangkok sand, Geomech. Energy Environ. 20 (2019) 100127, https://doi.org/10.1016/j.gete.2019.100127.
[56] M. Rafai, A.M. Tang, T. Badinier, J. de Sauvage, D. Salciarini, Effect of thermal cycles on sand-concrete interface under constant shear stress, Can. Geotech. J. (2024), https://doi.org/10.1139/cgj-2023-0140.
[57] S. Morteza Zeinali, S.L. Abdelaziz, Thermal consolidation theory, J. Geotech. Geoenviron. Eng. 147 (1) (2021) 04020147, https://doi.org/10.1061/(ASCE)GT.1943-5606.0002423.
[58] C.W.W. Ng, C. Shi, A. Gunawan, L. Laloui, Centrifuge modelling of energy piles subjected to heating and cooling cycles in clay, Géotech. Lett. 4 (2014) 310–316.
[59] P.J. Vardon, J. Peuchen, CPT correlations for thermal properties of soils, Acta Geotech 16 (2021) 635–646, https://doi.org/10.1007/s11440-020-01027-2.
[60] NEN NPR 7201:2017 Geotechniek, Bepaling Van Het Axiaal Draagvermogen Van Funderingspalen Door Middel Van Proefbelasting, 2017.
[61] A. Lupattelli, E. Cernuto, B. Brunelli, E. Cattoni, D. Salciarini, Experimentation of the Thermo-Mechanical Behavior of the Soil-Concrete Interface, Springer Series in Geomechanics and Geoengineering, 2023, pp. 343–350.
[62] Y. Guo, A. Golchin, M.A. Hicks, S. Liu, G. Zhang, P.J. Vardon, Experimental investigation of soil–structure interface behaviour under monotonic and cyclic thermal loading, Acta Geotech 18 (2023) 3585–3608, https://doi.org/10.1007/s11440-022-01781-5.
[63] H.L. Liu, C.L. Wang, G.Q. Kong, A. Bouazza, Ultimate bearing capacity of energy piles in dry and saturated sand, Acta Geotech 14 (2019) 869–879, https://doi.org/10.1007/s11440-018-0661-6.
[64] S.L. Abdelaziz, T.Y. Ozudogru, Non uniform thermal strains and stresses in energy piles, Environ Geotech 3 (4) (2016) 237–252, https://doi.org/10.1680/jenge.15.00032.
[65] G. Kong, J. Fang, X. Huang, H. Liu, H. Abuel-Naga, Thermal induced horizontal earth pressure changes of pipe energy piles under multiple heating cycles, Geomech Energy Environ 26 (2021) 100228, https://doi.org/10.1016/j.gete.2020.100228.